

# EVALUATION OF THE PERFORMANCE OF CLAY-BASED BRICKS WITH THE ADDITION OF CO-COMBUSTION ASH

LEA ŽIBRET,<sup>1</sup> IVANA CAREVIĆ,<sup>2</sup> NINA ŠTIRMER,<sup>2</sup>  
IVAN KOLODA,<sup>3</sup> MOJCA VRČON MIHELJ,<sup>4</sup>  
MIHA KRAGELJ,<sup>4</sup> VILMA DUCMAN<sup>1</sup>

<sup>1</sup> Slovenian National Building and Civil Engineering Institute, Ljubljana, Slovenia  
lea.zibret@zag.si, vilma.ducman@zag.si

<sup>2</sup> University of Zagreb, Faculty of Civil Engineering, Zagreb, Croatia  
ivana.carevic@grad.unizg.hr, nina.stirmer@grad.unizg.hr

<sup>3</sup> NEXE, Dilj d.o.o., Vinkovci, Croatia  
ivan.koloda@nexe.hr

<sup>4</sup> Goriške opekarne d.o.o., Renče, Slovenia  
mojca.vrcon@goriske.si, miha.kragelj@goriske.si

The gradual replacement of coal by local renewable resources leads to an increased production of co-combustion ashes (CC). Their disposal can be limited by their use in the construction sector, where they can partially replace primary raw materials. This study evaluates the incorporation of selected Slovenian CC ash into clay-based fired bricks within the EU AshCycle project. The tests included the measurement of water absorption, porosity, density, weight loss, shrinkage, flexural and compressive strength, and freeze-thaw resistance. Two types of clay were used to compare the influence of the selected ash on the performance of the fired samples. Replacing clay mixtures with 10 wt% CC ash reduced the compressive strength of the fired bricks but it still reached the required 10 MPa as specified in EN 772-1 (2015). The addition of CC ash to fired bricks requires careful planning of the raw mixes, taking into account various parameters that may affect the properties of the products.

DOI  
[https://doi.org/  
10.18690/um.fkkt.1.2025.15](https://doi.org/10.18690/um.fkkt.1.2025.15)

ISBN  
978-961-286-959-5

**Keywords:**  
fired clay bricks,  
waste ashes,  
raw mixture,  
ceramic-technological tests,  
freeze-thaw resistance



University of Maribor Press

## 1 Introduction

Worldwide large amounts of biomass ashes are landfilled (Insam and Knapp 2011). In accordance with the global initiatives on the gradual replacing of the fossil fuels by the renewable resources coal-combustion power plants are introducing a biomass as supplementary fuel (Sahu et al. 2014). The resulting co-combustion (CC) ashes may have various applications. One of the largest global industries, which could consume large amounts of co-combustion ashes, is brick making.

Fired clay bricks are one of the most versatile building materials in the world. Clay for brick production can be at least partially replaced by various secondary raw materials, such as dredged sediments (Božič et al. 2023), sawdust (Cultrone et al. 2020), wastewater treatment sludge (Detho et al. 2024), slags and various ashes (Zhang 2013): coal ash (Zhang 2013), MSWI ash (Haiying et al. 2011; Kirkelund et al. 2020), sewage sludge ash (Ottosen et al. 2020) and biomass ash (Eliche-Quesada et al. 2017; Šantek Bajto and Štirmer 2019). On the other hand clay supplies are limited and already running out in some parts of the world and consequently promoting the circular economy model seems crucial for the future of the brick sector (Zhang 2013). Furthermore, firing the mixture of clay and secondary raw materials at around 1000 °C can significantly reduce the leaching of heavy metals from the secondary raw materials (Ukwatta and Mohajerani 2017) what can be of importance also when utilize waste ash in clay bricks production to avoid disposal to landfills, which leads to a reduction in the cost of ash treatment and brick production (Haiying et al. 2011).

Fired bricks are usually produced by a vacuum extrusion, which ensures a homogeneous and dense structure (Krakowiak et al. 2011; Božič et al. 2023). Extruded brick samples can also be produced on a laboratory scale, which allows a direct comparison of industrial and laboratory samples (Viani et al. 2018). On the other hand, the final properties of fired bricks are strongly influenced by the composition of the raw mix. The high proportion of carbonates in the raw brick mix leads to increased weight loss during firing at temperatures of up to 950 °C and increased porosity of the fired bricks, which weakens their mechanical properties (Božič et al. 2023). Similar to carbonates, biomass ash is known as a pore-forming additive that increases the porosity of fired bricks and can contribute to the deterioration of mechanical properties (Beal et al. 2019).

As part of the EU project AshCycle - *Integration of underutilized ashes into material cycles by Industry-Urban symbiosis*, ashes from various Slovenian incineration plants were tested for their potential use in fired clay bricks. A screening of ash replacement and firing temperature in the production of extruded bricks was carried out by measuring water absorption, porosity, density, weight loss, shrinkage, flexural and compressive strength and freeze-thaw resistance. In this study two different clay mixtures were used to compare the influence of the selected CC ash on the performance of the fired samples.

## **2 Materials and methods**

The raw materials included two types of basic clay mixes: (i) a mixture of marl (50 wt%), clay (48 %) and coal (2 wt%), provided by Goriške opekarne d.o.o. brick factory (GO) (ii) pure clay, provided by NEXE brick factory, Dilj d.o.o. (NA). The replacement of both basic clay mixes by 10 mass percent (ma%) of selected Slovenian biomass ash from the co-combustion of brown coal and wood biomass was investigated.

The particle size distribution (PSD) of ash and clays was measured by laser diffraction granulometry using a Sync+FlowSync laser particle size analyzer (Microtrack MRB) in wet dispersion measurement mode. The dispersion medium for the ash was isopropanol, while the clays were analyzed in distilled water with the addition of a dispersant. The ash was sieved to a particle size of less than 0.25 mm for this measurement.

The chemical composition of the raw materials was determined with an ARL PERFORM<sup>X</sup> sequential X-ray fluorescence (XRF) spectrometer (Thermo Fisher Scientific Inc., Ecublens, Switzerland) using UniQuant 5 software (Thermo Fisher Scientific Inc., Waltham, MA, USA). The samples were previously ignited at 950°C for 2 hours and then mixed with Fluxana (Li tetraborate and Li metaborate in a 1:1 mass ratio) at a ratio of 1:10 and melted into discs. LiBr(l) (50 mL H<sub>2</sub>O and 7.5 g LiBr(s) from Sigma Aldrich) was added to the mixture to prevent the melt from sticking to the Pt crucible.

The mineralogical composition of raw materials and bricks was performed using a PANalytical Empyrean X-ray diffractometer with CuK $\alpha$  radiation (wavelength CuK $\alpha$ 1 1.54 Å). The samples were ground to a particle size below 63  $\mu$ m. Each sample was measured from  $2\theta = 4^\circ$  to  $70^\circ$  with an increment of  $0.0130^\circ$  as it was rotated. The X-ray tube was operated at 45 kV and 40 mA. Phase determination was performed using PANalytical X'Pert High Score Plus Diffraction software v. 4.8. using the structures for the phases from the ICDD PDF 4 + 2016 RDB powder diffraction files.

The brick mixtures were prepared according to Table 1. Approximately 20 kg of each mixture was shaped in three main shapes using a laboratory vacuum extruder (Karl Händle & Söhne Mühlacker, type PZVMga): cylinders (mould diameter=56.3 mm; extruded length=55 mm), prisms (mould dimensions: 54.3 mm $\times$ 27.7 mm; extruded length=150 mm) and tiles (mould dimensions: 57.2 mm $\times$ 9.3 mm; extruded length=150 mm). Extruded shapes were fired in a chamber furnace at 950 °C, with a heating rate of 150 °C/h and a dwelling time of 2h.

The compressive strength was measured on fired cylinders using a ToniNORM (ToniTechnik, Berlin, Germany) at a force rate of 0.5 kN/s, while the bending strength was measured on fired prisms using a Gabbrielli tile strength tester (Gabbrielli, s.r.l., Calenzano, Italy). Compressive strength was measured on five specimens and bending strength on seven specimens (both results are average values). Drying and firing shrinkage was calculated from the difference in the length of the 50 mm lines impressed on the fresh prisms before/after firing (seven samples, two measurements for each; the reported result is an average of 14 values). The density of the fired prisms was calculated from the measured dimensions and mass. Water absorption was determined after the prisms had been boiled in water for two hours (the cooled samples were weighed). Freeze-thaw resistance was determined according to SIST EN 539-2 (2013). The samples were dried at  $(110 \pm 5)$  °C, pre-saturated by gradual immersion in water and subjected to 150 freeze/thaw cycles in a temperature range between  $(-16 \pm 3)$  °C and  $(+13 \pm 3)$  °C.

Extruded tiles were cut into smaller samples (57.2 mm  $\times$  9.3 mm  $\times$  25 mm) for firing in the gradient furnace. The samples were heated to 1134 °C at a heating rate of 150 °C/h and a dwelling time of 20 minutes. The water absorption of the samples fired in the gradient furnace was determined after gradual immersion in distilled water

(immersion of  $\frac{1}{4}$  of the length per hour, 4 hours) and subsequent boiling for two hours.

Samples of extruded bricks were cast in epoxy resin and dry polished. The prepared polished cross-sections were coated with a carbon layer of approximately 15 nm thickness and examined by SEM and EDXS using a JEOL IT500 LV SEM equipped with an Ultim Max detector (Oxford Instruments) operated in high vacuum mode with an accelerating voltage of 15 kV. EDXS was performed using Aztec 5.0 SP1 software (Oxford Instruments Nanotechnology Tools Ltd).

**Table 1: The extruded mixtures.**

sample designation	CC ash (wt%)	clay GO (wt%)	clay NA (wt%)
G-O	-	100	-
G-1	10	90	-
N-0	-	-	100
N-1	10	-	90

### 3 Results and discussion

#### 3.1 Characterization of the raw materials

Clay GO had the finest granulation with the highest percentage of particles less than 2  $\mu\text{m}$  in diameter. However, the GO clay also had some larger particles, whereas the Našice clay had a unimodal distribution. The CC ash had a similar distribution to the GO clay, but with a lower percentage of particles smaller than 2  $\mu\text{m}$  (Figure 1).

The mineralogical composition of the raw materials is shown in Figure 2. Both clays contained illite/muscovite, chlorite, feldspars and quartz. The NA clay showed higher intensities of clay minerals than the GO clay. Clay mix GO had an intense calcite peak related to the marl content (Figure 2). This was also evident in the chemical composition, namely clay mix GO had a higher CaO content compared to clay mix NA (Table 2). The main crystal phases of CC ash were quartz, calcite, anhydrite, lime, periclase and hematite, with minor amounts of brownmillerite and portlandite.

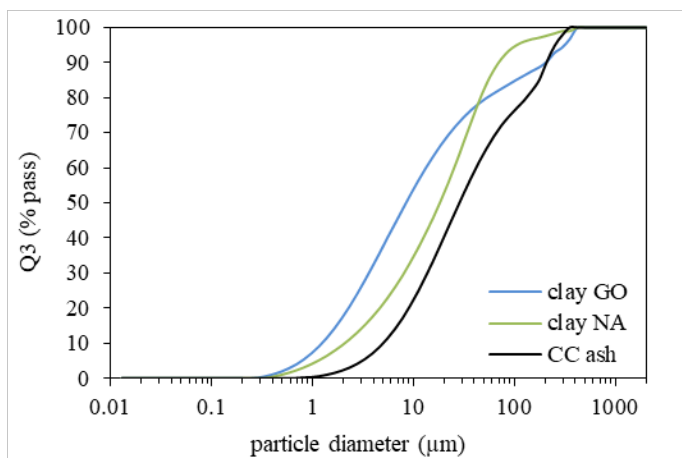


Figure 1: Cumulative particle size distribution (PSD) of clay mixes (clay GO, clay NA) and co-combustion (CC) ash, determined by laser diffraction.

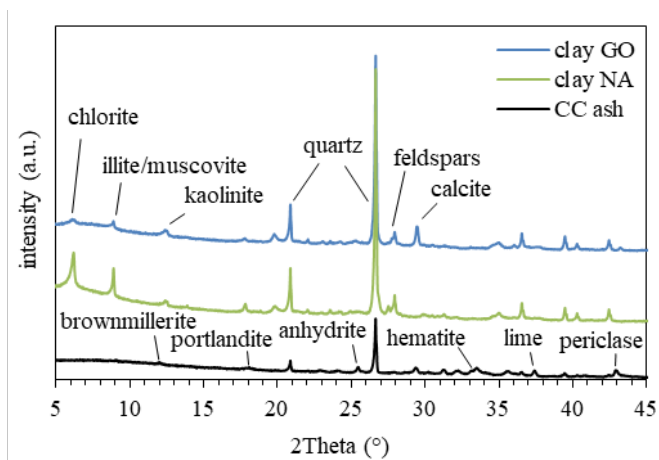


Figure 2: XRD patterns of clay mixes (clay GO, clay NA) and co-combustion (CC) ash.

Table 2: Chemical composition of raw materials measured by XRF (LOI = loss on ignition at 950 °C).

units	LOI	Na <sub>2</sub> O	MgO	Al <sub>2</sub> O <sub>3</sub>	SiO <sub>2</sub>	SO <sub>3</sub>	K <sub>2</sub> O	CaO	TiO <sub>2</sub>	Fe <sub>2</sub> O <sub>3</sub>	other
	wt%	wt%	wt%	wt%	wt%	wt%	wt%	wt%	wt%	wt%	wt%
clay GO	8.97	0.84	1.71	15.63	59.04	0.20	2.24	4.07	0.70	6.00	0.61
clay NA	6.22	1.07	1.40	16.77	64.35	b.d.l.	2.17	0.84	0.95	5.57	0.66
CC ash	16.30	0.35	8.18	10.70	28.21	1.70	2.22	19.98	0.53	10.57	1.26

### 3.2 Ceramic technological tests

The physical and mechanical properties of the bricks after drying and firing at 950 °C are shown in Table 3. Mixture N-0 had a higher drying shrinkage than mixture G-0. The 10 wt% replacement of clay GO with ash resulted in a lower drying shrinkage, while for clay Našice a 10 wt % ash did not significantly change the drying shrinkage of the samples, despite the high water demand (moisture content) of mixture N-1 (Table 3).

The effect of the firing temperature on shrinkage and water absorption is shown in Figure 3. The mixtures with clay NA showed a higher water absorption and lower firing shrinkage than mixtures with clay GO. For example, the shrinkage and water absorption of the pure clay NA sample (sample N-0) at 940 °C were 0.0% and 13.9%, while the shrinkage and water absorption of the sample with clay GO (sample G-0) at 940 °C were 1.0% and 13.0%. The water absorption increased significantly when 10 wt % CC ash was incorporated into both mixtures. Thus, the water absorption of the clay NA sample (sample N-1) at 940 °C was 23.2%, while the water absorption of the sample with clay GO (sample G-1) at 940 °C was 20.5%. The firing shrinkage was only slightly lower the when clay mixtures were replaced by 10 wt % CC ash.

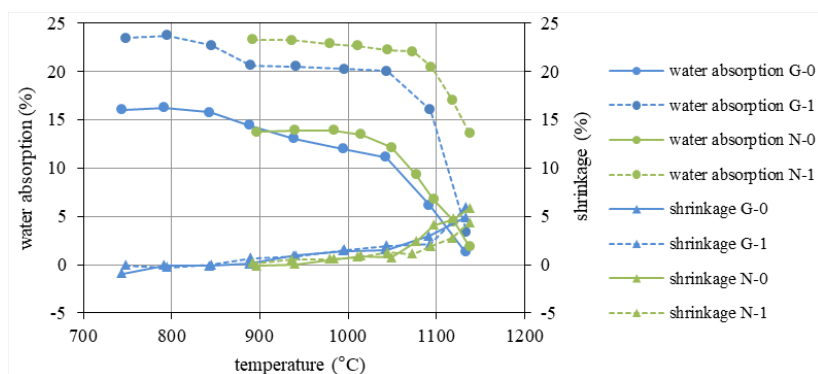


Figure 3: Water absorption and shrinkage of the samples, fired in gradient kiln.

The fired sample G-0 (with marl) had a higher compressive and flexural strength than the fired sample N-0, which did not contain marl. However, when clay mixes were replaced by 10 wt % CC ash, the G-1 bricks (with marl) had a slightly lower

compressive strength than the N-1 bricks. Incorporated ash reduced the density of the fired products, regardless of the clay type (Table 3).

**Table 3: Properties of bricks after drying and firing at 950 °C and freeze-thaw resistance.**

	CC ash (wt %)	moist. per wet mass during extrusion (%)	drying shrink. by length (%)	firing shrink. by length (%)	water absorption (%)	density (g/cm <sup>3</sup> )	bending strength (MPa)	compressive strength (MPa)	freeze/thaw resistance
<b>G-0</b>	0	18.8	7.8	0.2	11.8	1.89	17	72.6	yes
<b>G-1</b>	10	21.6	5.6	0.2	21.5	1.63	6.9	27.3	yes
<b>N-0</b>	0	20.4	9.2	0.7	13.3	1.88	12.7	42.1	yes
<b>N-1</b>	10	25.8	9.3	0.1	23.2	1.6	5.6	34.7	no

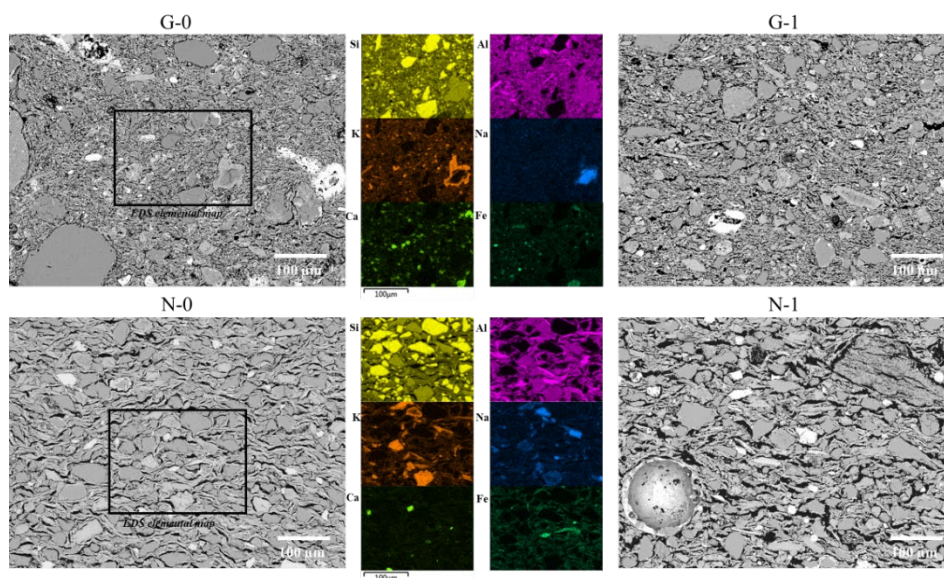


**Figure 4: SEM micrographs of the fired bricks and EDXS elemental maps for the selected areas.**

The fired bricks N-0 and N-1 showed a higher open porosity than G-0 and G-1 (Figure 4). Electron microscopy confirmed the increased porosity of the sample N-0 and N-1 compared to samples G-0 and G-1 (Figure 4). The homogeneously distributed elongated pores in N-0 and N-1 are most likely due to the higher clay mineral content in the clay mixture NA (Figure 2) and the shrinkage associated with the evaporation of physically bound water in clay. Sample N-1 had the highest open porosity (Table 3). As a result, the thinnest N-1 specimens (tiles) cracked during

room drying and were the source of new surface cracks during the freeze/thaw test (Table 3, Figure 5). In addition, the clay mix NA with 10 wt% ash (N-1) was very difficult to knead and required high moisture (Table 3), as the ash content of 10 wt% is too high for this type of clay. Nevertheless, the compressive strengths of all samples exceeded the 10 MPa limit specified in EN 772-1(2015).

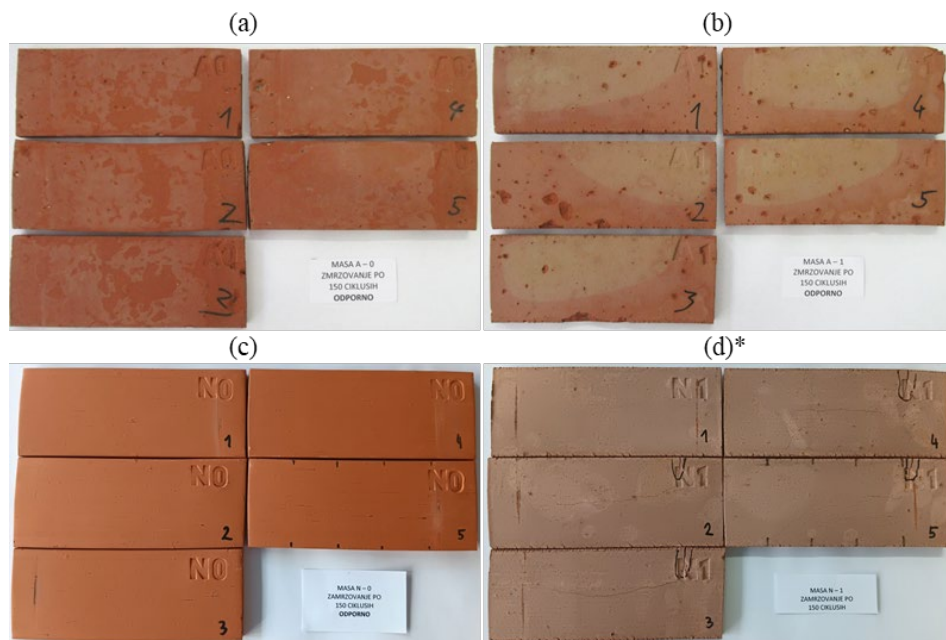


Figure 5: Bricks, fired at 950 °C, after 150 freeze/thaw cycles: (a) G-0, (a) G-1, (c) N-0, (d) N-1. \* The circled cracks were formed during drying and are not related to freeze/thaw deformation.

#### 4 Conclusions

Although the replacement of pure clay or clay with marl by 10 wt% CC ash reduced the compressive strength of the fired bricks, it was still above the 10 MPa limit specified in EN 772-1 (2015). The reduction in strength was less when pure clay was used than when clay with marl was used. However, the mixture of pure clay with 10 wt% ash was very difficult to knead as the ash content of 10 wt% is too high for this type of clay. Higher clay mineral content promoted shrinkage associated with evaporation of physically bound water in the clay. This resulted in cracking during

drying and poorer freeze-thaw resistance. The incorporation of CC ash into fired bricks requires careful design of the raw mixtures, taking into account various factors that can affect the properties of the products.

### Acknowledgments

This research has received funding from the European Union under the AshCycle project, grant agreement no. 101058162, and partial support from the Slovenian Research and Innovation Agency (ARIS) under research core grant no. P2-0273.

### Data availability

The data presented in this study are openly available from the repository DiRRROS at link: <http://hdl.handle.net/20.500.12556/DiRRROS-20922>.

### References

- Beal, B., Selby, A., Atwater, C., James, C., Viens, C., Almquist, C. (2019). A Comparison of Thermal and Mechanical Properties of Clay Bricks Prepared with Three Different Pore-Forming Additives: Vermiculite, Wood Ash, and Sawdust. *Environmental Progress and Sustainable Energy* 38, 13150. <https://doi.org/10.1002/ep.13150>
- Božič, M., Žibret, L., Kvočka, D., Pranjic, A. M., Gregorc, B., Ducman, V. (2023). Drava river sediment in clay brick production: Characterization, properties, and environmental performance. *Journal of Building Engineering* 71, 106470. <https://doi.org/10.1016/j.jobee.2023.106470>
- Cultrone, G., Aurrekoetxea, I., Casado, C., Arizzi, A. (2020). Sawdust recycling in the production of lightweight bricks: How the amount of additive and the firing temperature influence the physical properties of the bricks. *Construction and Building Materials* 235, 117436. <https://doi.org/10.1016/j.conbuildmat.2019.117436>
- Detho, A., Kadir, A. A., Ahmad, S. (2024). Utilization of wastewater treatment sludge in the production of fired clay bricks: An approach towards sustainable development. *Results in Engineering* 21, 101708. <https://doi.org/10.1016/j.rineng.2023.101708>
- Eliche-Quesada, D., Felipe-Sesé, M. A., Martínez-Martínez, S., Pérez-Villarejo, L. (2017). Comparative Study of the Use of Different Biomass Bottom Ash in the Manufacture of Ceramic Bricks. *Journal of Materials in Civil Engineering* 29, 04017238. [https://doi.org/10.1061/\(ASCE\)MT.1943-5533.0002078](https://doi.org/10.1061/(ASCE)MT.1943-5533.0002078)
- Haiying, Z., Youcai, Z., Jingyu, Q. (2011). Utilization of municipal solid waste incineration (MSWI) fly ash in ceramic brick: Product characterization and environmental toxicity. *Waste Management* 31, 331–341. <https://doi.org/10.1016/j.wasman.2010.10.017>
- Insam, H., Knapp, B. A. (eds) (2011). Recycling of Biomass Ashes. *Springer Berlin Heidelberg, Berlin, Heidelberg*
- Kirkelund, G. M., Skevi, L., Ottosen, L. M. (2020). Electrodialytically treated MSWI fly ash use in clay bricks. *Construction and Building Materials* 254, 119286. <https://doi.org/10.1016/j.conbuildmat.2020.119286>
- Krakowiak, K. J., Lourenço, P. B., Ulm, F. J. (2011). Multitechnique Investigation of Extruded Clay Brick Microstructure. *Journal of the American Ceramic Society* 94, 3012–3022. <https://doi.org/10.1111/j.1551-2916.2011.04484.x>

- Ottosen, L. M., Bertelsen, I. M. G., Jensen, P. E., Kirkelund, G. M. (2020). Sewage sludge ash as resource for phosphorous and material for clay brick manufacturing. *Construction and Building Materials* 249, 118684. <https://doi.org/10.1016/j.conbuildmat.2020.118684>
- Sahu, S. G., Chakraborty, N., Sarkar, P. (2014). Coal–biomass co-combustion: An overview. *Renewable and Sustainable Energy Reviews* 39, 575–586. <https://doi.org/10.1016/j.rser.2014.07.106>
- Šantek Bajto, J., Štirmer, N. (2019). Possibilities of wood biomass ash use in brick production. In: *5th Symposium on Doctoral Studies in Civil Engineering, University of Zagreb Faculty of Civil Engineering*, pp 81–93
- Ukwatta, A., Mohajerani, A. (2017). Leachate analysis of green and fired-clay bricks incorporated with biosolids. *Waste Management* 66, 134–144. <https://doi.org/10.1016/j.wasman.2017.04.041>
- Viani, A., Ševčík, R., Appavou, M. S., Radulescu, A. (2018). Evolution of fine microstructure during firing of extruded clays: A small angle neutron scattering study. *Applied Clay Science* 166, 1–8. <https://doi.org/10.1016/j.clay.2018.09.002>
- Zhang, L. (2013). Production of bricks from waste materials – A review. *Construction and Building Materials* 47, 643–655. <https://doi.org/10.1016/j.conbuildmat.2013.05.043>
- (2013) SIST EN 539-2. Clay roofing tiles for discontinuous laying-Determination of physical characteristics-Part 2: Test for frost resistance
- (2015) SIST EN 772-1. Methods of test for masonry units Determination of compressive strength

